Available Online: 19 January 2026 DOI: 10.54254/3049-5458/2026.31387

Predicting immunotherapy outcomes in breast cancer: a model leveraging copper metabolism signatures

*Ying Zhong, Yongyu He, Xiaodong Zhang**

Department of Gastrointestinal and Gland Surgery, The First Affiliated Hospital of Guangxi, Nanning, China

*Corresponding Author. Email: 15177788067@163.com

Abstract. Background: Copper ions play multiple roles in cancer metastasis and invasion. Breast cancer prognosis and immunotherapy efficacy are intricately linked with genes associated with copper metabolism. Studies have shown the therapeutic potential of eliminating or overloading copper ions in cancer. Further study is needed to elucidate the correlation between copper ion metabolism and cancer progression. Methods: Based on The Cancer Genome Atlas (TCGA) dataset, this study first performed univariate COX regression and LASSO regression analyses on 111 copper metabolism-related genes. Subsequently, patients were stratified into high- and low-risk groups, and systematic comparisons were conducted between the two groups in terms of clinical stratification, immune cell infiltration, tumor mutational burden, and predicted immunotherapy response. To further validate the clinical relevance of the model genes, this study analyzed their protein expression patterns using the Human Protein Atlas database and performed immunohistochemical experiments with clinical breast cancer tissues and matched adjacent normal samples for confirmation. Results: A prognostic model was created to predict using the lasso-Cox regression results and the genes DLAT, SLC31A1, LOXL1, and MTF1. The low copper metabolism gene score group showed better survival outcomes, while the high copper metabolism gene score group was associated with enhanced immunotherapy response. Immunohistochemical staining revealed high DLAT, SLC31A1, LOXL1, and MTF1 protein expression. Conclusion: This work highlights the profound impact of copper metabolism on breast cancer biology, linking it to patient survival, immune landscape, and therapeutic response. These insights have direct implications for developing predictive biomarkers to guide personalized immunotherapy. The results provide a new perspective for breast cancer treatment and may offer a basis for optimizing diagnosis and treatment strategies.

Keywords: copper metabolism model, immunotherapy prognosis, breast cancer

1. Introduction

Breast cancer remains a major clinical oncology challenge due to its high heterogeneity and evolving therapeutic paradigms. Although multimodal strategies—including surgery, chemotherapy, radiotherapy, and targeted therapy—have led to considerable progress, achieving durable remission and improving survival outcomes remains an ongoing effort, particularly for patients with advanced or treatment-resistant disease. The history of cancer treatment is a narrative of innovation, transitioning from cytotoxic agents to the new era of

Copyright: © 2026 by the authors. Submitted for possible open access publication under the terms and conditions of the Creative Commons Attribution (CC BY) license (https://creativecommons.org/licenses/by/4.0/).

precision medicine and immunotherapy. This evolution underscores a critical need: not only to develop novel therapeutics but also to identify reliable predictive biomarkers that can guide treatment decisions [1, 2].

In recent years, breast cancer management has been revolutionized by molecular subtyping and the emergence of immunotherapies. Established frameworks such as the intrinsic PAM50 molecular subtypes and PD-L1 expression scoring and PLK1 expression levels provide crucial prognostic and predictive guidance for modern therapeutic strategies [1, 3, 4]. The advent of immune checkpoint inhibitors has fundamentally reshaped the therapeutic paradigm for a wide range of solid tumors [1, 5]. Mounting research suggests that the microbiome profile may function as a reliable biomarker to stratify patients based on their likely response to immunotherapeutic agents [6]. The clinical application of immune checkpoint inhibitors in breast cancer faces two major challenges: first, their efficacy is largely confined to specific subtypes—for example, triple-negative breast cancer; second, innate or acquired resistance is commonly observed among patients. A key contributor to this resistance is the immunosuppressive tumor microenvironment (TME), which undermines effective anti-tumor immunity. Thus, elucidating the mechanisms that shape an immunosuppressive TME is essential for developing strategies to overcome immunotherapy resistance.

Concurrently, an emerging and captivating area of research explores how cellular metabolism fundamentally shapes these dual processes. Among various metabolic pathways, copper homeostasis has recently attracted significant attention. Pivotal in fundamental biological processes such as mitochondrial respiration and antioxidant defense, copper acts as an indispensable trace element and key enzymatic activator. However, dysregulated copper metabolism—common in cancers—promotes oncogenic signaling, angiogenesis, and metastasis, a phenomenon termed "cuproplasia". The recent elucidation of the cuproptosis mechanism directly reveals that copper can function both as an indispensable micronutrient for life and as a cytotoxic effector molecule. Cuproptosis, triggered by the aggregation of lipoylated proteins in the mitochondrial TCA cycle, has brought copper metabolism to the forefront of oncological research. Numerous pan-cancer studies have demonstrated that dysregulated copper flux and cuproptosis regulators not only carry prognostic value but are also closely associated with immune infiltration across various malignancies—from clear cell renal cell carcinoma to glioma—revealing a potential therapeutic vulnerability in cancers with disrupted redox circuits [1, 7].

This study aims to link these two critical areas by examining how copper levels sculpt breast cancer immunology. We propose that genes controlling copper balance alter local immunity and, in turn, treatment outcomes. Using data from TCGA and ICGC, we initially developed a prognostic model derived from copper-associated genes. We further demonstrate that this signature not only predicts patient survival but is also strongly correlated with distinct immune features within the TME. Our findings establish copper metabolism as a novel regulator of the breast cancer immune microenvironment and a promising predictor of immunotherapy response, offering fresh perspectives for overcoming treatment resistance.

Building upon this emerging paradigm and consistent with existing studies that have utilized TCGA data mining and LASSO regression to establish associations between cuproptosis and biomarkers in cancers such as glioma and hepatocellular carcinoma, particularly highlighting strong links with MTF1, DLAT, and SLC31A1 [8, 9]. We hypothesize that a cuproptosis-related gene signature can risk-stratify BRCA patients and elucidate the crosstalk between copper metabolism and the immune TME. Although prior TCGA-based studies have successfully employed similar approaches to decipher oncogenic pathways, we acknowledge the inherent technical and biological biases of bulk transcriptomic databases, which necessitate cautious interpretation of the findings [10, 11].

Furthermore, we explore the translational potential of our results, considering the future possibility of detecting these copper metabolism-related biomarkers in circulating components via liquid biopsy that

strategy already successfully used in other cancers for dynamic monitoring [12]. This could translate our mechanistic insights into clinically applicable tools for dynamic patient management and early detection.

2. Materials and methods

2.1. Materials

The rabbit-derived polyclonal antibodies against DLAT (A04469-2), SLC31A1 (BA2421), LOXL1 (PB0758), and MTF1 (A04733-3), and goat anti-rabbit IgG secondary antibodies were purchased from BOSTER Company (China). The HRP-labeled goat anti-rabbit IgG secondary antibody (GB23303) was purchased from Servicebio (China). The blocking goat serum (SL038) was purchased from Solarbio (China).

2.2. Methods

2.2.1. Acquisition of copper metabolism-associated genes

From MSigDB version 7.5.1, we compiled a comprehensive list of 111 copper metabolism-associated genes [13]. and incorporating previously identified regulatory genes for copper-induced cell death [14] (Table S1).

2.2.2. Dataset and data processing

We obtained BRCA data from TCGA and ICGC databases (https://dcc.icgc.org/). The TCGA dataset contained 957 tumor and 102 normal samples, while the ICGC dataset comprised 1010 tumor samples. Preparation for analysis involved converting all dataset expression values to TPM format. From TCGA, we retrieved RNA sequencing results along with patient clinical details, then excluded duplicates and cases with missing clinical data. Following normalization to TPM, the processed expression data were merged with the curated clinical dataset. Differential gene expression analysis was performed using the "DESeq2" R package. Following this, survival analysis was conducted with the "survival" package, and time-dependent ROC curves were generated using the "survivalROC" package to evaluate predictive performance.

2.2.3. Prediction model establishment and validation

The LASSO regression technique was employed to construct the prognostic model, while the "glmnet" package was used to identify high-dimensional prognostic genes. The data were analyzed using the "glmnet" package, which generated two key lambda values: λ.min and λ.1se. Upon selecting the λ.min value, the model demonstrated superior predictive performance. hereby mitigating overfitting.

$$Risk\ Score = (DLAT * 0.170950592) + (SLC31A1 * 0.147188976) + (LOXL1 * -0.110429075) + (MTF1 * 0.019163801) \quad (1)$$

where exprgenei represents the TPM value and coefficientgenei denotes its corresponding lasso coefficient.

This equation was used to compute the risk score for each patient with BRCA. Subsequently, the samples were classified into high-risk or low-risk groups, thereby adhering to the rigorous standards of Nature.

2.2.4. Nomogram construction

To enhance model accuracy across internal and external cohorts, we employed a predictive tool developed with the rms package and assessed its performance via calibration and discrimination metrics.

2.2.5. Immune spectrum analysis

To assess the immune status and predictive characteristics of cohorts with high or low scores for copper-associated genes, we employed the "CIBERSORT" package [15]. A methodical approach for the comprehensive analysis and comparative assessment of immune composition in these two cohorts was taken. Furthermore, This study utilized the ESTIMATE algorithm to calculate stromal content, immune infiltration

levels, tumor purity, and an integrated tumor microenvironment score for each sample [1, 16]. We further utilized the TIDE approach [17] to obtain TIDE scores for the probability of tumor immune evasion in both cohorts.

2.2.6. Mutation landscape

Mutation information from 957 patients with BRCA was acquired from TCGA database via cBioPortal [18]. The mutation data were examined utilizing the "maftools" [19] R package. TMB score was derived from the "maftools" package.

2.2.7. Drug sensitivity analysis

Drug sensitivity analysis was conducted using the R package "oncoPredict" in conjunction with the GDSC database (Genomics of Drug Sensitivity in Cancer), which focuses specifically on genomic features related to cancer drug response [20]. Using transcriptomic data from BRCA samples, comprehensive analysis was performed to assess treatment efficacy by predicting drug sensitivity in patients with diverse scoring profiles.

2.2.8. Protein expression by the Human Protein Atlas (HPA) database

The HPA encompassed specimens derived from 46 distinct healthy human tissues and over 20 types of human malignancies, all of which were immunolabeled using antibodies targeting more than 11,000 human proteins [21]. The laser power and detector gain parameters configured during image acquisition defined four staining intensity categories: negative, weak positive, moderate positive, and strong positive [22].

2.2.9. Tissue specimens and patient information

Based on the World Health Organization (WHO) 2023 histopathological diagnostic criteria for gastrointestinal adenocarcinoma, we collected five surgical specimens pathologically diagnosed as BRCA (breast cancer) by the hospital's Department of Pathology. None of the enrolled patients had undergone prior chemotherapy or immunotherapy. None of the enrolled patients had undergone prior chemotherapy or immunotherapy. The protocol was approved by the institutional ethics committee (2024-E048-01) and conducted in accordance with the Declaration of Helsinki. Written informed consent was obtained from all participants.. Immunohistochemical analysis was conducted on the tissue sections obtained from these surgical specimens. Immunohistochemistry was performed on the cancer and adjacent tissue from each patient. Typical images of each tissue section and four representative tumor cell areas were randomly captured for analysis at 50x magnification. The immunohistochemical staining intensity of LOXL1, MTF1, DLAT, SLC31A1 was analyzed using Image J software. Protein expression was quantified as Area (%). The results demonstrated that the levels of LOXL1, MTF1, DLAT, and SLC31A1 genes in cancer tissues were significantly higher than those in adjacent normal tissues. The Area (%) values of the 14 groups of samples was compared using a Student’s t-test.

2.3. Statistical analysis

All statistical analyses were carried out in R (version 4.2.3). Group comparisons were conducted via Student’s t test, Wilcoxon test, and Kruskal–Wallis test. A P value < 0.05 was considered statistically significant and is denoted by asterisks in figures.

3. Results

3.1. Identifying potential prognostic genes linked to copper metabolism in TCGA-BRCA dataset

Based on the copper metabolism-related gene set, univariate COX regression analysis identified 13 genes significantly associated with patient survival (the technical roadmap is detailed in Supplementary Figure 1).

The heatmap results in Figure 1A show that, compared with normal tissues, the levels of DLD, MMGT1, DLAT and GPC1 genes were downregulated in tumor tissues, while the expression of the remaining genes showed an upregulated trend. The enrichment analysis (Figure 1B) demonstrated that these genes predominantly participate in copper ion binding, transition/metal ion transmembrane transport, and NAD/NADP-dependent aldehyde/ketone oxidoreductase activity ($P < 0.01$).

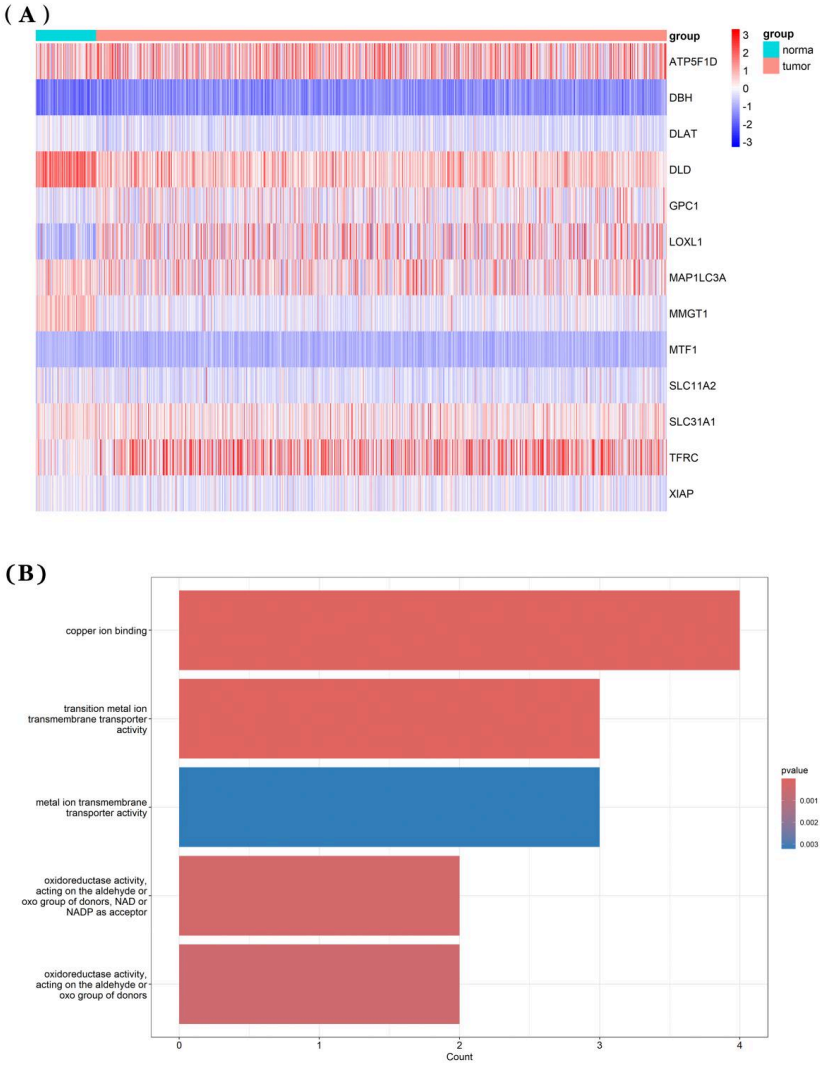

Figure 1. Heatmap of the expression of 13 genes in the normal and tumor groups (A).Enriched Gene Ontology terms associated with 13 DEGs (B)

3.2. Construction and validation of a prognostic model for copper metabolism

To improve the precision of gene identification and establish a predictive model, we conducted lasso regression analysis on the aforementioned 13 genes. This revealed that the model achieved the best fit when utilizing 10 genes and a λ value of 0.004921004 (Figure 2A, B). The single-factor Cox regression analysis and lasso regression coefficients for these 10 genes, which were used to construct the prognostic model, are

summarized in Table 1. $DLAT$, $SLC31A1$, $LOXL1$, and $MTF1$ were chosen to construct the prognostic model, using the following formula:

$$Risk\ Score = (DLAT * 0.170950592) + (SLC31A1 * 0.147188976) + (LOXL1 * -0.110429075) + (MTF1 * 0.019163801) \quad (2)$$

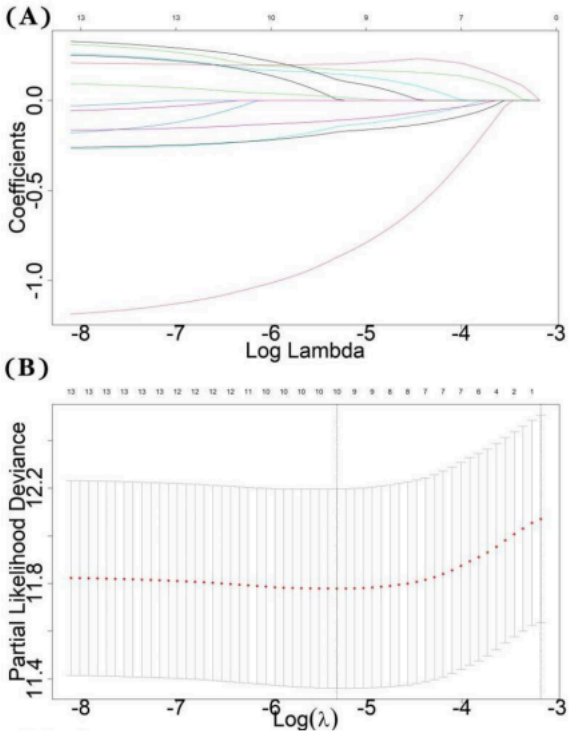

Figure 2. (A) By LASSO analysis, 10 genes were screened out and λ was 0.004921004 at the minimum partial likelihood deviation. (B) Path diagram of lasso regression coefficients.

Table 1. Univariate analysis results and LASSO coefficients of the 10 genes selected by LASSO

Univariate analysis result and Lasso coefficient				
gene	Uni_Coe	HR (95% CI Uni)	P_value_Uni	Lasso_Coe
ATP5F1D	-0.3193034	0.727 (0.575-0.919)	$p < 0.01$	0.007280226
DBH	-1.1540486	0.315 (0.148-0.671)	$p < 0.01$	-0.871242038
DLAT	0.6222982	1.863 (1.364-2.545)	$p < 0.01$	0.170950592
GPC1	-0.3137051	0.731 (0.586-0.911)	$p < 0.01$	-0.145031478
LOXL1	-0.2547666	0.775 (0.65-0.925)	$p < 0.01$	-0.110429075
MAP1LC3A	-0.3441745	0.709 (0.576-0.872)	$p < 0.01$	-0.174769515
MMGT1	0.5896890	1.803 (1.327-2.45)	$p < 0.01$	0.202058949
MTF1	0.4457172	1.562 (1.155-2.112)	$p < 0.01$	0.019163801
SLC31A1	0.4942496	1.639 (1.216-2.21)	$p < 0.01$	0.147188976
XIAP	0.4460530	1.562 (1.14-2.141)	$p < 0.01$	0.116371746

Figure 3A illustrates the contrasting profiles between high- and low-risk groups regarding survival outcomes (status and time) and the expression of relevant prognostic genes.

The distribution of risk scores in the TCGA cohort clearly delineates high- and low-risk groups. Specifically, individuals with elevated DLAT, SLC31A1, and MTF1 gene expression levels exhibited higher risk scores, whereas those with decreased LOXL1 gene expression had lower risk scores. Comparable gene expression patterns were also evident in the ICGC test set (Figure 3D).

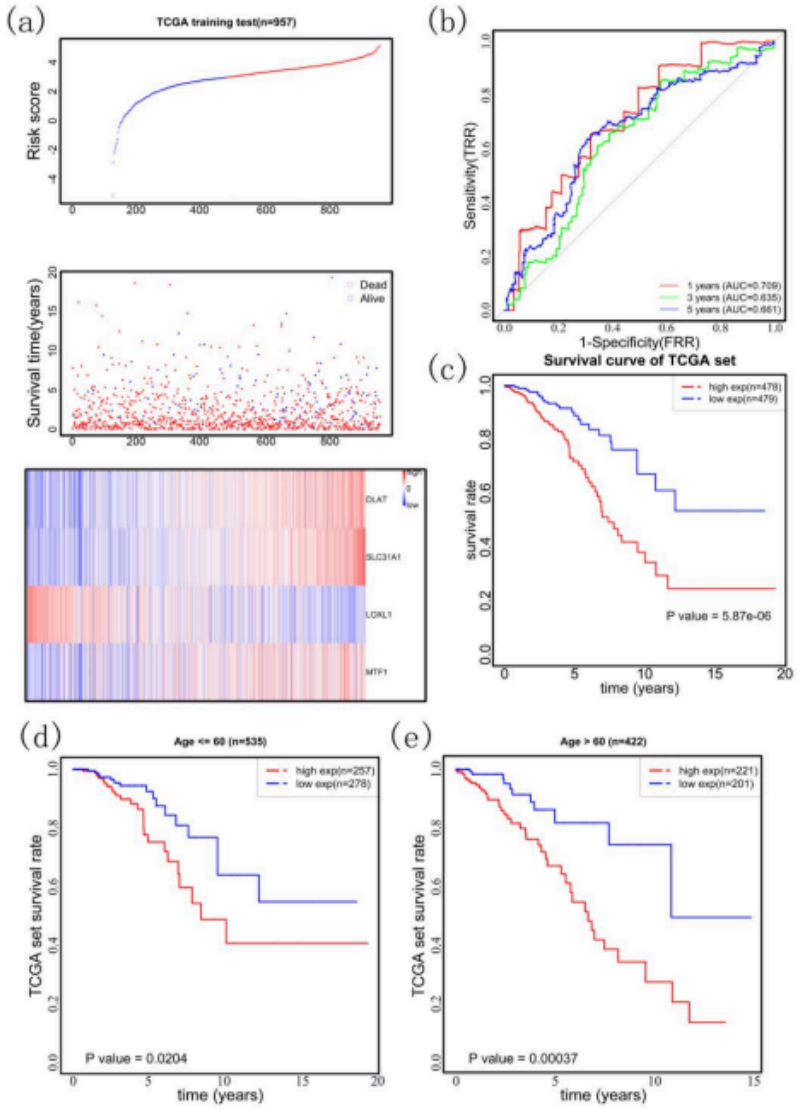

Figure 3. Predictive performance analysis of the prognostic model (A) Distribution of risk scores and Overall Survival (OS) in the training set and (D) the testing set, along with heatmaps showing the expressiong levels of prognostic genes. (B) Receiver Operating Characteristic (ROC) curves of the prognostic model for predicting 1, 3, and 5year OS in the training set and (E) the testing set. (C) KaplanMeier survival analysis comparing overall survival between the highrisk and lowrisk groups in the training set and (F) the testing set

To assess the prognostic relevance of gene signatures in BRCA, ROC analysis was performed. The corresponding AUCs for 1, 3, and 5year survival predictions in TCGA were 0.709, 0.635, and 0.661. Consistently, highrisk patients exhibited markedly reduced overall survival relative to the lowrisk group ($P < 0.0001$, Figure 3C) Validation in the ICGC cohort demonstrated AUCs of 0.693, 0.643, and 0.670 for predicting survival at 1, 3, and 5 years (Figure 3E) and confirmed a persistently significant prognostic

separation between high and lowrisk patients ($P < 0.0001$, Figure 3F). These findings indicate that the gene marker exhibits stable prognostic predictive ability in both the training and validation sets. Further agestratified analysis demonstrated that the risk score maintained significant prognostic discriminatory power across different age subgroups ($P < 0.05$, Figures 4A–D).

Analyses for model independence, including univariate and multivariate Cox regression, consistently identified the risk score as an independent prognostic factor across both high- and low-risk groups. (Table 2).

Table 2. Univariate and multivariate COX analysis of RiskScore

Model independence evaluation table						
	Coeffcient	HR	lower 95	upper 95	*P* value	
Single factor cox regression analysis results						
age						
low age uni (< 65)	-0.005374366	0.99464005	0.965746131	0.024398439	0.720857345	ns
high age uni (≥ 65)	0.10468808	1.110364212	1.04986998	1.174344163	0.000249675	***
riskScore						
low risk	-0.832110574	0.435129943	0.246995012	0.76656636	0.003976078	**
high risk	-1.036942091	0.354537168	0.162784264	0.772166798	0.009027801	**
grade						
low grade uni (≤ 2)	0.789609664	2.20253653	1.554870421	3.119981639	8.82E-06	***
high grade uni (> 2)	0.398615319	1.489760426	0.980784358	2.2628686	0.061624125	ns
Multiariable cox regression analysis results						
age						
low age mul (< 65)	0.059714595	1.061533536	1.026823621	1.097416756	0.000430662	***
high age mul (≥ 65)	0.068954542	1.071387505	1.02224096	1.122896881	0.004000621	**
riskScore						
low risk	0.059714595	1.061533536	1.026823621	1.097416756	0.000430662	***
high risk	0.068954542	1.071387505	1.02224096	1.122896881	0.004000621	**
grade						
low grade mul (≤ 2)	0.059714595	1.061533536	1.026823621	1.097416756	0.000430662	***
high grade mul (> 2)	0.068954542	1.071387505	1.02224096	1.122896881	0.004000621	**

We also performed nomogram plot analysis, which demonstrated that a low CRG score confers a notable predictive advantage for long-term survival (Figure 4A).

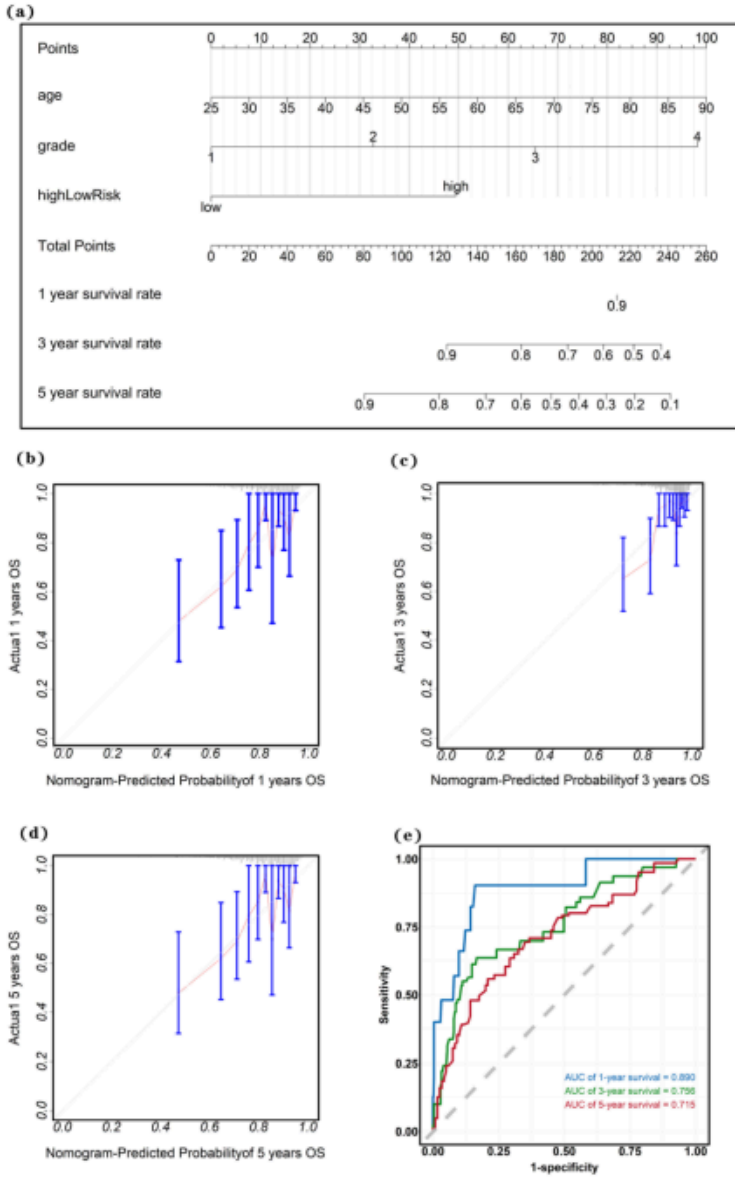

Figure 4. Construction and validation of the prognostic nomogram. (A) The nomogram was constructed by integrating independent risk factors screened by univariateCox regression. ROC curves of the nomogram in the (E) TCGA set. Calibration curves of the nomogram for predicting 1-, 3-, and 5-year OS in the (B-C) TCGA sets

The calibration curve (Figure 4E) validated the nomogram's predictive performance: AUCs reached 0.890 (1 year), 0.756 (3 year), and 0.715 (5 year) for survival prediction; additionally, predicted survival rates closely matched observed values across time points (Figures 4B–D).

3.3. Analysis of immune cell infiltration and mutation landscape

Tumor immunosuppression within the microenvironment is closely linked to breast cancer progression. To assess this relationship, we quantified four immune-associated features: tumor purity (Figure 5A), stromal (Figure 5B), immune (Figure 5C), and ESTIMATE (Figure 5D). Comparative analysis revealed that patients in the low-risk group exhibited significantly elevated stromal, immune, and ESTIMATE scores, in contrast to

markedly reduced tumor purity ($P < 0.0001$). These distinct immune profiles imply that copper ion metabolism likely contributes to breast cancer progression through its influence on the tumor immune microenvironment.

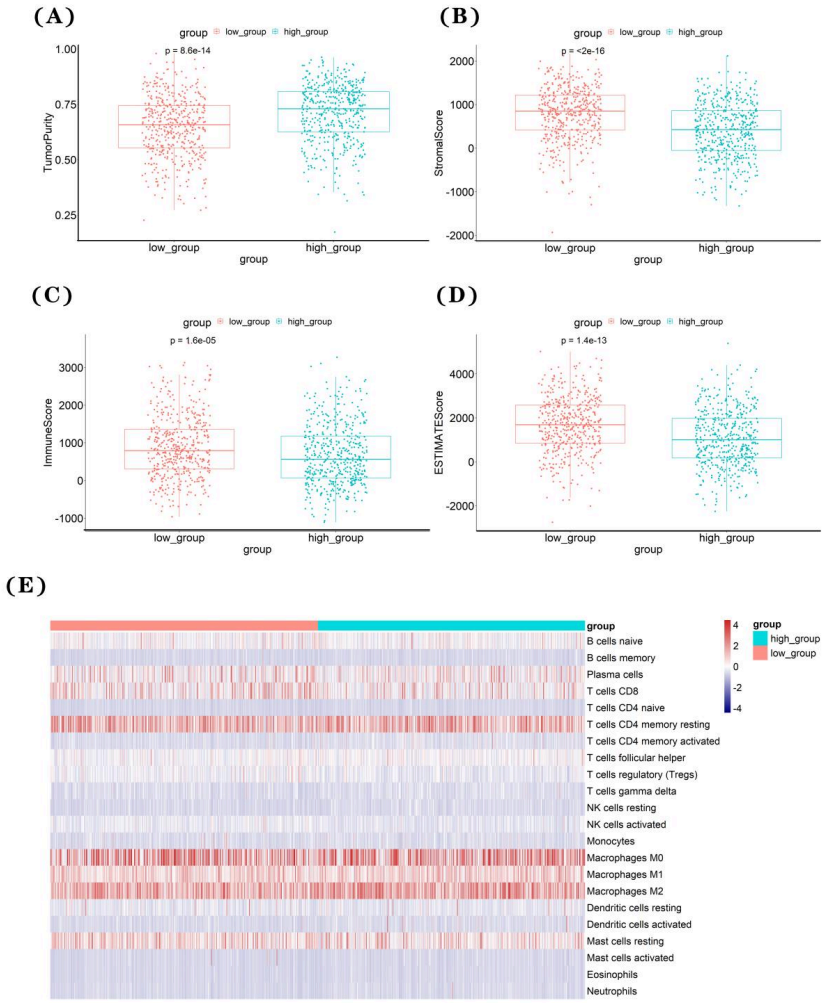

Figure 5. Tumor Purity (A), Stromal Score (B), Immune Score (C), and ESTIMATE Score (D). (E) Heatmap of immune cell infiltration

To further understand the tumor microenvironment in patient cohorts with high and low risk scores, we conducted comparative analysis of immune cell infiltration levels in TCGA dataset. Our findings, depicted in Figure 5E–6A, suggest that the high-risk group showed increased immune cell infiltration in the tumor tissue, including activated dendritic cells, M2 macrophages, neutrophils, resting NK cells, and CD4 memory-activated T cells ($P < 0.05$). These results underscore a significant association between the prognostic model of copper metabolism-related genes and the tumor microenvironment.

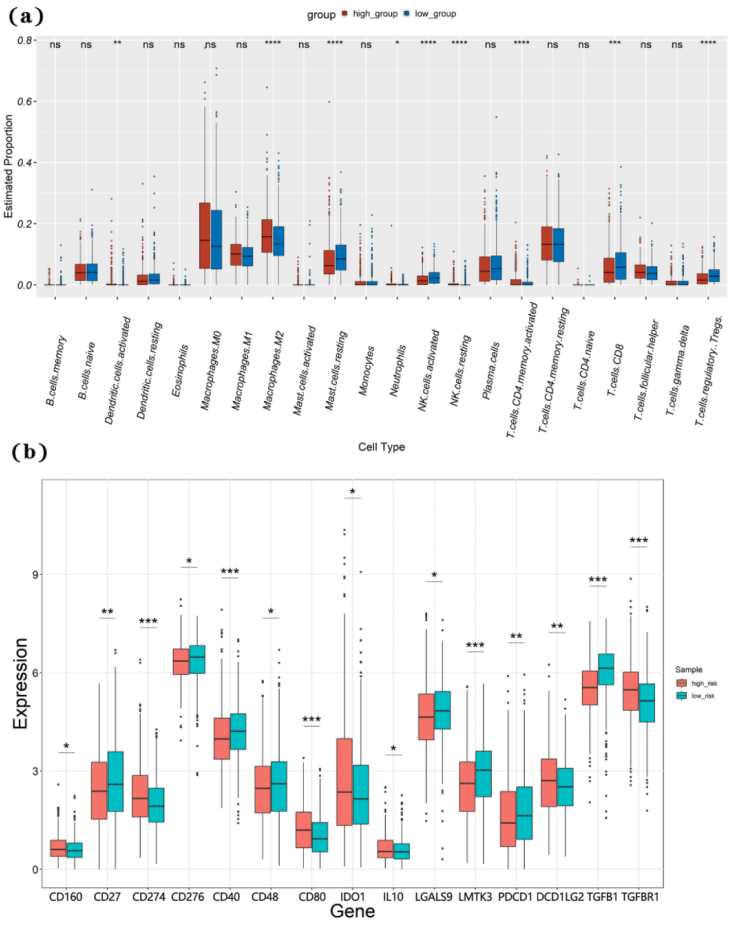

Figure 6. (A) Comparison of immune cell infiltration in the high and low risk groups. (B) Comparison of immune checkpoints between the the high and low risk groups. *$p < 0.05$; **$p < 0.01$; ***$p < 0.001$; ****$p < 0.0001$

Next, we explored the gene expression patterns linked to immune checkpoint modulation. As depicted in Figure 6B, the low-risk group demonstrated elevated immune checkpoint gene expression levels, such as CD27, CD276, CD40, CD48, LGALS9, LMTK3, PDCD1, and TGFB1. Conversely, the high-risk group exhibited increased immune checkpoint gene expression levels, including CD160, CD274, CD80, IDO1, IL10 and TGFBR1 ect ($P < 0.05$).

Increased immune checkpoint gene expression levels may suppress immune cell function and attenuate immune responses. Tumor cells can alter the TME by modulating immune checkpoint gene expression in both tumor and immune cells, thereby hindering anti-tumor immunity and facilitating immune evasion by tumor cells. This phenomenon may contribute to the disparate prognoses observed in the two high-risk groups. To investigate the prospective utility of the prognostic model in predicting immunotherapy efficacy, analysis was conducted on TCGA dataset. The prevalence of PIK3CA gene mutations was notable, constituting 85.54% of the observed mutation rate within the low-risk cohort (Figure 7A). In contrast, the high-risk group demonstrated a mutation rate of 81.78%, with the TP53 gene exhibiting the most prominent mutations (Figure 7B).

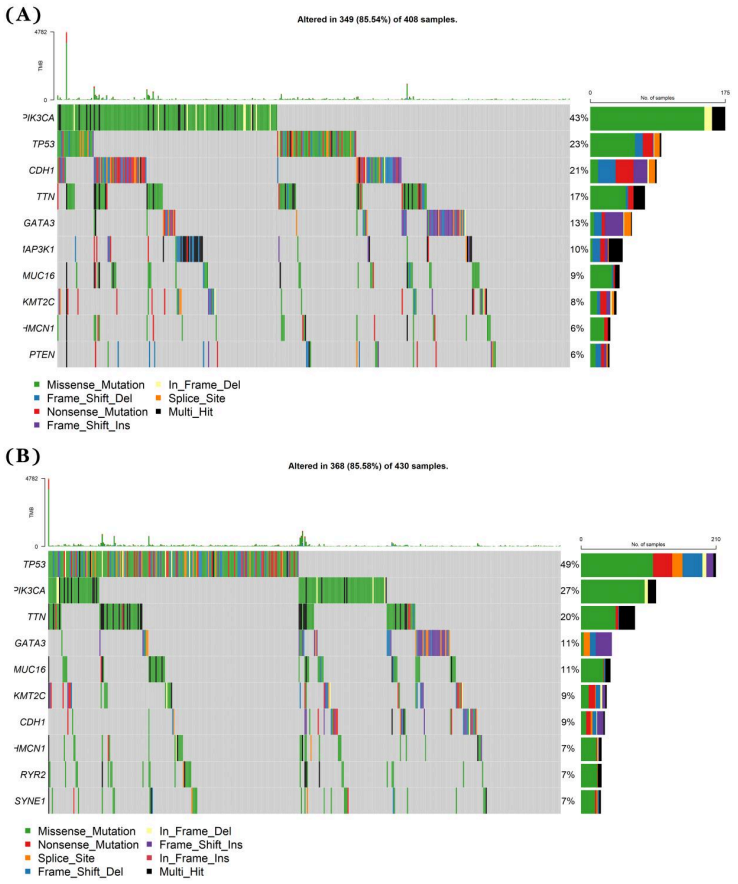

Figure 7. Mutational landscape of the low (A) and high (B) risk groups

3.4. Immunotherapy effect prediction

A significant positive correlation was observed (R = 0.18, P < 0.0001; Figure 8A), with the high-risk group exhibiting a significantly higher Tumor Mutational Burden (TMB) than the low-risk group (P < 0.0001; Figure 8B). These findings indicate that high-risk patients may have an enhanced likelihood of responding to immunotherapy.

The TIDE algorithm, which captures these features through tumor gene expression [23], can estimate immune escape likelihood and thus help predict efficacy of immune checkpoint blockade. To further examine immunotherapy benefit in high-risk patients, we evaluated tumor immune escape using TIDE. These results suggest the risk score may serve as a prognostic biomarker, with higher scores indicating a greater likelihood of immunotherapy response.

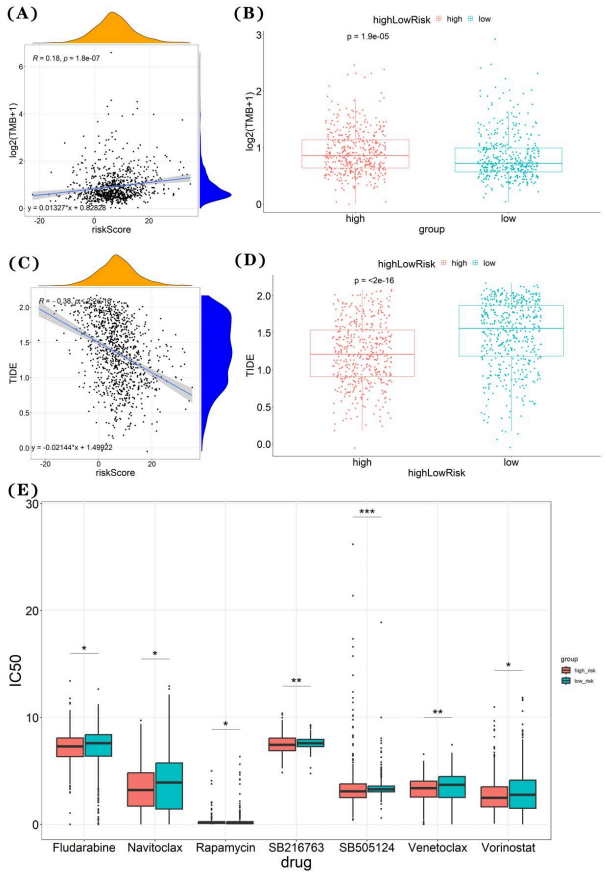

Figure 8. (A) Correlation between TMB and riskScores. *$p < 0.05$; **$p < 0.01$; ***$p < 0.001$; ****$P < 0.0001$. (B) Boxplot of TMB, compared by Wilcox.test. (C) Correlation between TIDE and riskScores. *$p < 0.05$; **$p < 0.01$; ***$p < 0.001$; ****$P < 0.0001$. (D) Boxplot of TIDE in the low-risk group and high-risk group, compared by Wilcox.test. (E) Comparison of drug sensitivity

3.5. Prediction of treatment outcomes in groups with different scores

Statistical comparison of drug sensitivity scores between groups revealed significantly reduced values in the lower-scoring cohort ($P < 0.05$). Predicted sensitivity profiles indicated that seven agents—fludarabine, navitoclax, rapamycin, SB216763, SB505124, venetoclax, and vorinostat—exhibited markedly lower sensitivity scores ($P < 0.05$; Figure 8E). Conversely, this suggests that high-risk patients may demonstrate greater therapeutic responsiveness to these drugs.

3.6. Identifying abnormal gene expression in BRCA samples through immunohistochemical analysis

We first queried these genes in the HPA database (Figure 9).This revealed the presence of MTF1, DLAT, and SLC31A1 protein in BRCA samples. MTF1 and DLAT protein exhibited moderate and low expression levels, respectively, in the majority of BRCA samples, whereas SLC31A1 protein had weak expression in most BRCA samples.

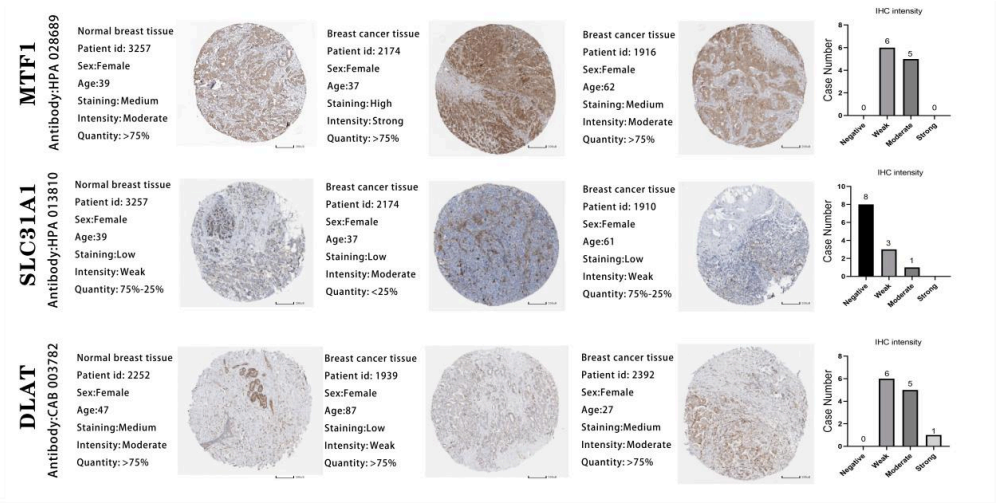

Figure 9. Expressions of MTF1, DLAT, and SLC31A1 protein in BRCA. (A) Representative IHC images of MTF1, SLC31A1, and DLAT from the HPA database, analyzing the clinical samples of normal and tumor tissues included in it. Bar charts summarize immunohistochemical staining intensities for MTF1 (11 patients), SLC31A1 (12 patients), and DLAT (12 patients). Scale Bar = 200 μm

3.7. Immunohistochemistry

We selected the LOXL1,MTF1,DLAT and SLC31A1 gene for validation. Immunohistochemistry was performed on the cancer and adjacent tissue from 30 patients with BRCA. Figure 10A shows representative images for each tissue section and four representative tumor cell areas. The expression levels of MTF1, DLAT, SLC31A1 and LOXL1 were significantly higher in tumor tissues compared with adjacent normal tissues. (Figure 10B).

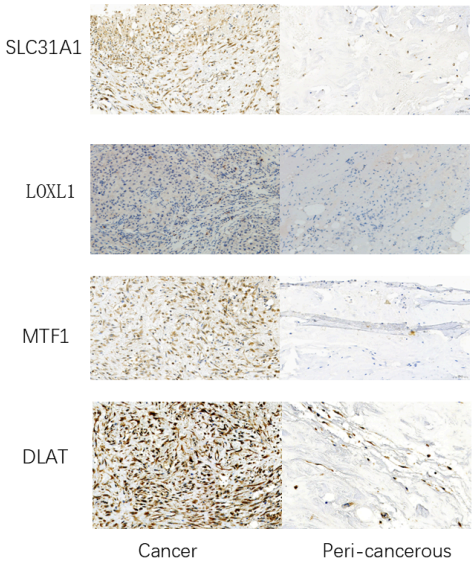

(A)

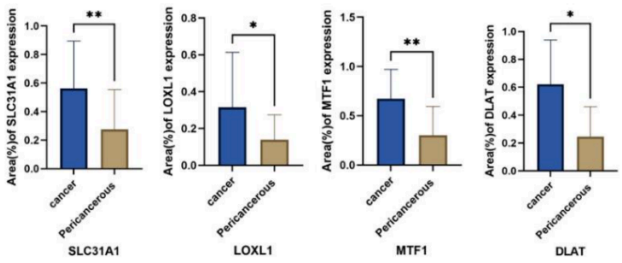

(B)

Figure 10. (A) LOXL1, MTF1, DLAT and SLC31A1 expression in normal and tumors breast tissue. Normal tissue was collected from the negative margin adjacent to the tumor. Representative images of immunohistological analysis. Scale Bar = 50μm. (B) The expression levels of MTF1, DLAT, SLC31A1 and LOXL1 were significantly higher in tumor tissues compared with adjacent normal tissues. (Student's t test). *$p < 0.05$; **$p < 0.01$; ***$p < 0.001$: **** $p < 0.0006$

4. Discussion

Leveraging data from TCGA-BRCA and ICGC cohorts, we systematically examined the influence of copper metabolism on BRCA progression and the tumor microenvironment (TME). A copper metabolism-associated gene signature comprising LOXL1, MTF1, DLAT, and SLC31A1 was constructed using a training cohort and validated in an independent test cohort. Assessment across multiple clinicopathological parameters revealed significantly worse outcomes in signature-defined high-risk patients. The risk score was further validated as an independent prognostic marker by both univariate and multivariate Cox regression. To optimize prognostic stratification, we constructed a composite nomogram integrating risk score, tumor grade, and age. Agestratified validation further demonstrated that the prognostic efficacy of the risk score was not affected by age. Distinct immune profiles differentiated the risk groups: high-risk patients exhibited increased tumor mutational burden and decreased TIDE scores, implying greater tumor immunogenicity and likely immunotherapy sensitivity. Moreover, risk scores positively correlated with enhanced response to immune checkpoint blockade. Together, the copper metabolism-based risk model offers a promising framework for personalizing immunotherapy strategies in breast cancer.

At a molecular level, SLC31A1 (CTR1) mediates cellular copper uptake by facilitating copper (I) import across the plasma membrane and chaperoning copper to binding partners such as ATOX1, thereby fine-tuning intracellular copper homeostasis [1, 24]. LOXL1 contributes to extracellular matrix remodeling in malignancy through collagen and elastin cross-linking [1, 25]. MTF1, a cysteine-rich metal-binding transcription factor, regulates gene expression in response to heavy metal exposure . Beyond MTF1-mediated resistance to copper chelation observed in vitro [26]. DLAT, as a key subunit of the pyruvate dehydrogenase complex, finetunes TCA cycle flux via sirtuin 4dependent deacylation and lysine biotinylation. In line with the Warburg effect, cancer cells exhibit heightened reliance on aerobic glycolysis, and DLAT may serve as a metabolic marker implicated in cancer progression and metastasis via regulation of pyruvate oxidation and glycolytic metabolism [1, 27] .

To date, the association between these four copper metabolism-related genes and BRCA pathogenicity has not been explicitly examined. Therefore, we interrogated the HPA database and employed experimental models to evaluate the protein and mRNA expression of SLC31A1, MTF1, DLAT, and LOXL1. Immunohistochemical analyses confirmed the upregulation of SLC31A1, MTF1, DLAT, and LOXL1 in

BRCA tissues compared with normal controls. Overall, our results suggest an important role for copper metabolic pathways in shaping the immunosuppressive TME and modulating response to immunotherapy in BRCA. The proposed risk model may hold clinical relevance for patient stratification, prognostication, and prediction of chemotherapy benefit. Furthermore, this work establishes a foundation for elucidating the mechanistic contributions of copper metabolism genes to BRCA progression.

While this study offers a comprehensive profile of copper metabolism in BRCA and identifies candidate therapeutic targets, several limitations must be acknowledged. Our analyses relied primarily on retrospective data from public repositories and a single institutional cohort. Although an internally validated nomogram was developed, external validation is necessary prior to clinical implementation. Further functional validation through in vitro and in vivo models, coupled with prospective longitudinal studies, is essential to confirm our findings. Most importantly, the precise molecular mechanisms through which copper ions and associated genes influence BRCA cell metabolism and immune evasion remain to be fully elucidated.

The emergence of liquid biopsy technologies has revolutionized non-invasive cancer monitoring, as evidenced by applications in neuroblastoma and other malignancies [12] . Should our identified copper metabolism-related genes be detectable in circulating tumor DNA (ctDNA) or extracellular vesicles, their incorporation into liquid biopsy panels may enable real-time tracking of pathway activity and early disease detection. Such translation could yield clinically actionable tools for dynamic risk assessment and management. Looking forward, evolving insights into tumor biology will continue to drive precision oncology approaches, particularly those targeting immune and metabolic vulnerabilities. Innovations in immunotherapy and metabolic intervention hold substantial promise, and therapeutic targeting of copper metabolism via copper chelation or inhibition of copper-dependent signaling may represent a novel strategy to impede tumor progression and improve outcomes in BRCA.

In the context of breast cancer, this shift means moving beyond traditional chemotherapy and radiation toward therapies tailored to individual genetic profiles and tumor microenvironment characteristics [28]. Notably, targeting copper metabolism-related genes represents a novel and promising avenue. Copper plays a crucial role in angiogenesis, metastasis, and signaling pathways in breast cancer. Therapies designed to modulate copper metabolism, such as copper chelators or drugs targeting copper-dependent enzymes could inhibit tumor growth and improve patient outcomes [29].

5. Conclusion

In brief, we have developed a predictive model for genes related to copper metabolism in BRCA: the first of its kind. This model facilitates accurate prognostication of patients with BRCA and prediction of their potential response to immunotherapy. Additionally, we have verified the atypical expression of SLC31A1, MTF1, DLAT, and LOXL1 in patients with BRCA, opening a new avenue to explore copper metabolism–induced cell death as a therapeutic strategy for breast cancer.

Acknowledgements

Not applicable.

Data availability statement

All data generated or analyzed during this study are included in this published article and its supplementary information files. Additional data are available from the corresponding author upon reasonable request.

Statements and Declarations

Ethics approval statement

The study involving human participants was approved by the Guangxi Medical University Ethics Review Committee.

Consent for publication

All authors of the manuscript have read and approved the final version. We agree to the publication of this work in Journal of Translational Medicine and confirm that the content has not been published elsewhere.

Conflict of interest disclosure

The authors declare that this study was conducted in the absence of any commercial or financial relationship that could be interpreted as a potential conflict of interest.

Funding project

The National Natural Science Foundation of China (82000807)

Authors' contributions

YZ participated in the preliminary experimental design, preliminary experiment, main experiment operation, data analysis, manuscript writing and revision. YY participated in data analysis, manuscript writing and revision. XD supervised the study, contributed to writing (review and editing), and confirmed the authenticity of all raw data. All authors read and approved the final manuscript.

References

[1] Luo, Y., Tian, W., Kang, D., Li, Y., Zhang, H., Wang, Y., Chen, X., Liu, J., & Li, Z. (2025). RNA modification gene WDR4 facilitates tumor progression and immunotherapy resistance in breast cancer. *Journal of Advanced Research, 72*, 333–351.https: //doi.org/10.1016/j.jare.2024.06.029

[2] Sonkin, D., Thomas, A., & Teicher, B. A. (2024). Cancer treatments: Past, present, and future. *Cancer Genetics,* 286–287, 18–24. https: //doi.org/10.1016/j.cancergen.2024.06.002

[3] Shen, J., Zhang, W., Jin, Q., Gong, F., Zhang, H., Xu, H., Li, J., Yao, H., Jiang, X., Yang, Y., Hong, L., Mei, J., Song, Y., & Zhou, S. (2023). Polo-like kinase 1 as a biomarker predicts the prognosis and immunotherapy of breast invasive carcinoma patients. *Oncology Research, 32*(2), 339–351.https: //doi.org/10.32604/or.2023.030887

[4] Parker, J. S., Mullins, M., Cheang, M. C. U., Leung, S., Voduc, D., Vickery, T., Davies, S., Fauron, C., He, X., Hu, Z., Quackenbush, J. F., Stijleman, I. J., Palazzo, J., Marron, J. S., Nobel, A. B., Mardis, E., Nielsen, T. O., Ellis, M. J., Perou, C. M., & Bernard, P. S. (2009). Supervised risk predictor of breast cancer based on intrinsic subtypes. *Journal of Clinical Oncology, 27*(8), 1160–1167.https: //doi.org/10.1200/JCO.2008.18.1370

[5] Ye, F., Dewanjee, S., Li, Y., Chen, R., Wang, L., Duan, Z., & Wang, G. (2023). Advancements in clinical aspects of targeted therapy and immunotherapy in breast cancer. *Molecular Cancer, 22*(1), 105.https: //doi.org/10.1186/s12943-023-01805-y

[6] Xie, J., Liu, M., Deng, X., Li, S., & Li, H. (2024). Gut microbiota reshapes cancer immunotherapy efficacy: Mechanisms and therapeutic strategies. *iMeta, 3*(1), e156.https: //doi.org/10.1002/imt2.156

[7] Liu, H. (2023). Expression and potential immune involvement of cuproptosis in kidney renal clear cell carcinoma. *Cancer Genetics,* 274–275, 21–25. https: //doi.org/10.1016/j.cancergen.2023.03.002

[8] Zhang, B., Xie, L., Liu, J., Liu, A., & He, M. (2023). Construction and validation of a cuproptosis-related prognostic model for glioblastoma. *Frontiers in Immunology, 14*, 1082974. https: //doi.org/10.3389/fimmu.2023.1082974

[9] Xu, S., Dong, K., Gao, R., Wang, Y., Feng, J., & Zhao, Y. (2023). Cuproptosis-related signature for clinical prognosis and immunotherapy sensitivity in hepatocellular carcinoma. *Journal of Cancer Research and Clinical Oncology, 149*(13), 12249–12263.https: //doi.org/10.1007/s00432-023-05099-x

[10] Liu, H., Li, Y., Karsidag, M., Tu, T., & Wang, P. (2025). Technical and Biological Biases in Bulk Transcriptomic Data Mining for Cancer Research. *Journal of Cancer, 16*(1), 34–43. https: //doi.org/10.7150/jca.100922

[11] Liu, H., Guo, Z., & Wang, P. (2024). Genetic expression in cancer research: Challenges and complexity. *Gene Reports, 37*(000). https: //doi.org/10.1016/j.genrep.2024.102042

[12] Jahangiri, L. (2024). Updates on liquid biopsies in neuroblastoma for treatment response, relapse and recurrence assessment. *Cancer Genetics,* 288–289, 32–39. https: //doi.org/10.1016/j.cancergen.2024.09.001

[13] Subramanian, A., Tamayo, P., Mootha, V. K., Mukherjee, S., Ebert, B. L., Gillette, M. A., Paulovich, A., Pomeroy, S. L., Golub, T. R., Lander, E. S., & Mesirov, J. P. (2005). Gene set enrichment analysis: A knowledge-based approach for interpreting genome-wide expression profiles. *Proceedings of the National Academy of Sciences, 102*(43), 15545–15550.https: //doi.org/10.1073/pnas.0506580102

[14] Guo, J., Cheng, J., Zheng, N., Zhang, X., Dai, X., Li, L., Sun, M. J., Huang, B., Zhang, H., & Wang, H. (2021). Copper Promotes Tumorigenesis by Activating the PDK1-AKT Oncogenic Pathway in a Copper Transporter 1 Dependent Manner. *Advanced Science, 8*(18), 2004303.https: //doi.org/10.1002/advs.202004303

[15] Jiang, P., Gu, S., Pan, D., Fu, J., Sahu, A., Hu, X., Li, Z., Traugh, N., Bu, X., Li, B., Liu, J., Freeman, G. J., Brown, M. A., Wucherpfennig, K. W., & Liu, X. S. (2018). Signatures of T cell dysfunction and exclusion predict cancer immunotherapy response. *Nature Medicine, 24*(10), 1550–1558.https: //doi.org/10.1038/s41591-018-0136-1

[16] Gao, J., Aksoy, B. A., Dogrusoz, U., Dresdner, G., Gross, B., Sumer, S. O., Sun, Y., Jacobsen, A., Sinha, R., Larsson, E., Cerami, E., Sander, C., & Schultz, N. (2013). Integrative Analysis of Complex Cancer Genomics and Clinical Profiles Using the cBioPortal. *Science Signaling, 6*(269), pl1.https: //doi.org/10.1126/scisignal.2004088

[17] Mayakonda, A., Lin, D.-C., Assenov, Y., Plass, C., & Koeffler, H. P. (2018). Maftools: efficient and comprehensive analysis of somatic variants in cancer. *Genome Research, 28*(11), 1747–1756.https: //doi.org/10.1101/gr.239244.118

[18] Maeser, D., Gruener, R. F., & Huang, R. S. (2021). oncoPredict: an R package for predicting in vivo or cancer patient drug response and biomarkers from cell line screening data. *Briefings in Bioinformatics, 22*(6).

[19] Uhlén, M., Fagerberg, L., Hallström, B. M., Lindskog, C., Oksvold, P., Mardinoglu, A., Sivertsson, Å., Kampf, C., Sjöstedt, E., Asplund, A., Olsson, I., Edlund, K., Lundberg, E., Navani, S., Szigyarto, C. A.-K., Odeberg, J., Djureinovic, D., Takanen, J. O., Hober, S., … Pontén, F. (2015). Tissue-based map of the human proteome. *Science, 347*(6220), 1260419.https: //doi.org/10.1126/science.1260419

[20] Asplund, A., Edqvist, P. H. D., Schwenk, J. M., & Pontén, F. (2012). Antibodies for profiling the human proteome—The Human Protein Atlas as a resource for cancer research. *Proteomics, 12*(13), 2067–2077.https: //doi.org/10.1002/pmic.201100504

[21] Sha, D., Jin, Z., Budczies, J., Kluck, K., Liersch, T., & Sinicrope, F. A. (2020). Tumor Mutational Burden as a Predictive Biomarker in Solid Tumors. *Cancer Discovery, 10*(12), 1808–1825.https: //doi.org/10.1158/2159-8290.CD-20-0522

[22] Azamjah, N., Soltan-Zadeh, Y., & Zayeri, F. (2019). Global Trend of Breast Cancer Mortality Rate: A 25-Year Study. *Asian Pacific Journal of Cancer Prevention, 20*(7), 2015–2020.

[23] Mayakonda, A., Lin, D.-C., Assenov, Y., Plass, C., & Koeffler, H. P. (2018). Maftools: efficient and comprehensive analysis of somatic variants in cancer. *Genome Research, 28*(11), 1747–1756.https: //doi.org/10.1101/gr.239244.118

[24] Maung, M. T., Carlson, A., Olea-Flores, M., Elkhadragy, L., Schachtschneider, K. M., Navarro-Tito, N., & Padilla-Benavides, T. (2021). The molecular and cellular basis of copper dysregulation and its relationship with human pathologies. *The FASEB Journal, 35*(9), e21810.https: //doi.org/10.1096/fj.202100771R

[25] Vallet, S. D., & Ricard-Blum, S. (2019). Lysyl oxidases: from enzyme activity to extracellular matrix cross-links. *Essays in Biochemistry, 63*(3), 349–364. https: //doi.org/10.1042/EBC20180074

[26] Zhang, C., Wang, S., Tang, H., Lai, R., Cai, Q., Su, Y., Wu, H., & Huang, Y. (2024). Prognostic and Immunological Role of Cuproptosis-Related Gene MTF1 in Pan-Cancer. *Journal of Cancer, 15*(17), 5786–5809.https: //doi.org/10.7150/jca.98749

[27] Mathias, R. A., Greco, T. M., Oberstein, A., Budayeva, H. G., Chakrabarti, R., Rowland, E. A., Kang, Y., Shenk, T., & Cristea, I. M. (2014). Sirtuin 4 is a lipoamidase regulating pyruvate dehydrogenase complex activity. *Cell, 159*(7), 1615–1625.

[28] Joshi, R. M., Telang, B., Soni, G., & Rane, P. (2024). Overview of perspectives on cancer, newer therapies, and future directions. *Oncology and Translational Medicine, 10*(3), 105–109.https: //doi.org/10.1097/OT9.0000000000000039

[29] Fang, C., Peng, Z., Sang, Y., Ren, Z., Ding, H., Yuan, H., & Hu, K. (2024). Copper in Cancer: from transition metal to potential target. *Human Cell, 37*(1), 85–100.https: //doi.org/10.1007/s13577-023-00985-5